A Novel Hypoxia-inducible Factor 1α Inhibitor KC7F2 Attenuates Oxygen-induced Retinal Neovascularization

Xiaoyu Tang, Kaixuan Cui, Xi Lu, Peiqi Wu, Shanshan Yu, Boyu Yang, Yue Xu, and Xiaoling Liang

State Key Laboratory of Ophthalmology, Zhongshan Ophthalmic Center, Sun Yat-sen University, Guangdong Provincial Key Laboratory of Ophthalmology and Visual Science, Guangzhou, China

Correspondence: Xiaoling Liang, State Key Laboratory of Ophthalmology, Zhongshan Ophthalmic Center, Sun Yat-sen University, 7 Jinsui Road, Guangzhou 510060, China; liangxlsums@qq.com.
Yue Xu, State Key Laboratory of Ophthalmology, Zhongshan Ophthalmic Center, Sun Yat-sen University, 7 Jinsui Road, Guangzhou 510060, China; xuyue57@mail.sysu.edu.cn.

XT, KC, and XL contributed equally to this work.

Received: September 7, 2021
Accepted: May 19, 2022
Published: June 13, 2022

Citation: Tang X, Cui K, Lu X, et al. A novel hypoxia-inducible factor 1α inhibitor KC7F2 attenuates oxygen-induced retinal neovascularization. *Invest Ophthalmol Vis Sci.* 2022;63(6):13. https://doi.org/10.1167/iovs.63.6.13

Purpose. KC7F2 is a novel molecule compound that can inhibit the translation of hypoxia-inducible factor 1α (HIF1α). It has been reported to exhibit potential antiangiogenic effect. We hypothesized that KC7F2 could inhibit oxygen-induced retinal neovascularization (RNV). The purpose of this study was to investigate this assumption.

Methods. Oxygen-induced retinopathy (OIR) models in C57BL/6J mice and Sprague-Dawley rats were used for in vivo study. After intraperitoneal injections of KC7F2, RNV was detected by immunofluorescence and hematoxylin and eosin staining. Retinal inflammation was explored by immunofluorescence. EdU incorporation assay, cell counting kit-8 assay, scratch test, transwell assay, and Matrigel assay were used to evaluate the effect of KC7F2 on the proliferation, migration and tube formation of human umbilical vein endothelial cells (HUVEC) induced by vascular endothelial growth factor (VEGF) in vitro. Protein expression was examined by Western blot.

Results. KC7F2 treatment (10 mg/kg/d) in OIR mice significantly attenuated pathological neovascularization and decreased the number of preretinal neovascular cell nuclei, without changing the avascular area, which showed the same trends in OIR rats. Consistently, after the KC7F2 intervention (10 μM), cell proliferation was inhibited in VEGF-induced HUVEC, which was in agreement with the trend observed in the retinas of OIR mice. Meanwhile, KC7F2 suppressed VEGF-induced HUVEC migration and tube formation, and decreased the density of leukocytes and microglia colocalizing neovascular areas in the retinas. Moreover, the HIF1α–VEGF pathway activated in retinas of OIR mice and hypoxia-induced HUVEC, was suppressed by KC7F2 treatment.

Conclusions. The current study revealed that KC7F2 was able to inhibit RNV effectively via HIF1α–VEGF pathway, suggesting that it might be an effective drug for RNV treatment.

Keywords: KC7F2, HIF1α inhibitor, retinal neovascularization, retinopathy of prematurity, HIF1α-VEGF pathway

Retinopathy of prematurity (ROP) is a leading cause of blinding eye diseases in children.[1,2] An epidemiological study found that ROP occurred in 31.9% of preterm infants with gestational age of less than 32 weeks, 19.0% of which needed treatment.[3] Retinal neovascularization (RNV) is one of the principal pathological features in ROP,[4,5] which is defined as a state where new pathologic vessels from existing capillaries in the retina usually breach the internal limiting membrane of the retina and grow into the vitreous.[6] RNV is prone to exudation, hemorrhage, and fibrosis, resulting in vitreous hemorrhage and tractional retinal detachment, ultimately causing visual impairment and even blindness.[7] Therefore, the inhibition of RNV is of great significance for ROP treatment.

Vascular endothelial growth factor (VEGF) is a key regulatory factor of physiological and pathological retinal angiogenesis.[8] Intravitreal injection of anti-VEGF agents is one of the major modalities for RNV-associated diseases treatment.[9–11] However, to acquire better therapeutic effects, most patients require multiple injections, which increases the risk of injecting complications such as postoperative intraocular hypertension[12] and retinal detachment.[13] Moreover, because VEGF has neuroprotective and neurotrophic effects in retina, the treatment of anti-VEGF may lead to retinal neurodegeneration and decreased visual function.[14,15] Considering these issues, it is necessary to explore new and safer therapies to control pathological angiogenesis in retinopathy.

Hypoxia-inducible factor 1 (HIF1) is known as a heterodimeric protein complex, which consists of an oxygen dependent α subunit and a constitutively expressed β unit.[16] Under normoxia, HIF1α is hydroxylated by prolyl hydroxylases and degraded, whereas with hypoxia, the inhibited activity of prolyl hydroxylases results in stabilization of HIF1α, which translocates into the nucleus, binds to HIF1β, then initiates the transcription of angiogenic factors (e.g., VEGF, angiopoietin 2).[17] Substantial evidence indicates that the accumulation of HIF1α in hypoxic retina contributes to the formation of RNV.[7,18–20] Thus, the inhibition of HIF1α might be a valuable therapeutic strategy for the treatment of ROP.

KC7F2, a small-molecule compound with a central structure of cystamine, presents the ability of inhibiting HIF1α translation, which is likely caused by a decrease in the phosphorylation of translational repressor eIF4E binding protein and the ribosomal kinase S6K.[21] Initially, KC7F2 was developed as a cancer treatment. This antitumor effect of KC7F2 effectively targeted rapidly proliferating tumor cells, which resulted in deprivation of oxygen, causing hypoxia.[21,22] Previous studies have found that KC7F2 could inhibit angiogenesis and tumor cell invasion in a variety of malignant tumors, such as osteosarcoma and breast cancer.[23,24] To date, there has been little evidence that KC7F2 has a therapeutic effect on RNV, and its underlying molecular mechanisms need to be elucidated.

This study aimed to test the hypothesis that KC7F2 could inhibit RNV and explore the potential mechanisms, using rodent oxygen-induced retinopathy (OIR) models and human umbilical vein endothelial cell (HUVEC) treated with VEGF or hypoxia.

Methods

Reagents

Dulbecco's modified Eagle medium/nutrient mixture F12 medium, fetal bovine serum, PBS solution, 0.25% trypsin EDTA solution, and penicillin/streptomycin solution were purchased from Gibco BRL (Grand Island, NY). We purchased 4′,6-Diamidino-2-phenylindole (#C1006) was purchased from Beyotime Biotechnology (Shanghai, China). The antibodies used in this study are listed in Supplementary Table S1 and S2.

KC7F2 Administration

KC7F2 was purchased from Selleck Chemicals (Houston, TX, #S7946), dissolved by dimethyl sulfoxide (Sigma, St Louis, MO). For in vitro experiments, mother solution was freshly dilated to 10 µM with culture medium (dimethyl sulfoxide <0.1%), which did not affect the viability of HUVEC in preliminary experiments. For in vivo experiments, working solution was freshly made using PBS solution at a final concentration of 0.5% dimethyl sulfoxide, and intraperitoneally injected into mice (10 mg/kg/d) from postnatal day 12 (P12) to P17, which was referred to a previous study.[25] The doses for the rats (7 mg/kg/d, from P14 to P18) can be converted from the mouse dose according to the body surface area formula.

Rodent OIR Models

C57BL/6J mice and Sprague–Dawley rats were obtained from the Animal Laboratory of Zhongshan Ophthalmic Center (Guangzhou, China). OIR experiments were performed as previously described.[26,27] Details of OIR models were provided in the Supplementary Figure 1A and 1B. To account for possible litter-specific differences, each experimental group obtained from at least three different litters and the number of pups per litter was controlled (6–8 mice per litter, 12–14 rats per litter). All animal experiments complied with the ARVO Statement for the Use of Animals in Ophthalmic and Vision Research, and were approved by the Institutional Animal Care and Use Committee of Zhongshan Ophthalmic Center.

Immunofluorescence Assay

Immunofluorescent staining of whole retinal mounts, frozen sections, and HUVEC was performed as described previously.[28,29] All fluorescence images were taken using confocal laser scanning microscopy (LSM880, Carl Zeiss, Jena, Germany). For whole retinal mounts, six retinas were analyzed per experimental group and the extent of neovascular or avascular area were expressed as the percentage of the number of pixels in the neovascular tuft area/ avascular area relative to the number of pixels in the total retinal area. For frozen sections, six fields of view (at $\times$400 magnification) on each section were observed. Three sections were assessed from one eye per animal and at least six animals were used for each group. To minimize subjective bias, the quantitations of the neovascular and avascular areas and positive cells were conducted in a masked fashion by two experienced investigators not involved in the experimental design. Disagreements were determined by a third person after careful assessment.

Hematoxylin and Eosin (HE) Staining

The eyeballs in each group of mice were enucleated to make paraffin sections. HE staining was applied as described previously.[28] Sections were imaged using a light microscope (Leica, Frankfurt, Germany) to measure the number of vitreoretinal neovascular cells nuclei. A quantitative approach to HE staining kept consistent with what was detailed elsewhere in this article for the quantitation of the frozen sections.

HUVEC Culture and Treatment

HUVECs purchased from FuHeng Biology (Shanghai, China) were a pool derived from three donors, which were authenticated by short tandem repeat profiling. The cells were fed by Dulbecco's modified Eagle medium/F12 with 10% fetal bovine serum, and 1% penicillin/streptomycin and maintained at 37°C in a humidified atmosphere of 5% CO_2 and 95% air.

The interventions to HUVEC included two parts, namely, VEGF treatment and hypoxia treatment. Referring to the pervious study,[30] human recombinant VEGF165 protein (R&D Systems, Minneapolis, MN, #293-VE-010/CF) was added to a final concentration of 10 ng/mL for cell treatment. For VEGF stimulation test, HUVEC were divided into four groups: (i) control, HUVEC cultured in Dulbecco's modified Eagle medium/F1 with 10% fetal bovine serum; (ii) KC7F2, HUVEC treated 10 µM KC7F2 for 12 hours; (iii) VEGF, HUVEC treated 10 ng/mL VEGF for 12 hours; and (iv) VEGF + KC7F2, HUVEC treated with 10 µM KC7F2 and 10 ng/mL VEGF for 12 hours. For hypoxic stimulation test, HUVEC were divided into four groups: (i) control and (ii) KC7F2 were described elsewhere in this article; (iii) hypoxia, HUVEC cultured in a hypoxic incubator (Hua Yi Ning Chuang, Ningbo, China) adjusted to 1% O_2 for 12 hours; and (iv) hypoxia + KC7F2, on the basis of the hypoxia group, HUVEC treated with 10 µM KC7F2.

Cell Viability and Proliferation Assay

Cell counting kit-8 (CCK8, GLPBIO, Montclair, CA, #GK10001) assay was used to determine cell viability. HUVEC were seeded into 96-well plates at 5×10^3 per well for 12 hours. After being processed as described elsewhere

Investigative Ophthalmology & Visual Science

in this article, subsequent procedures were performed according to the manufacturer's instructions.

An EdU incorporation assay (Click-iT EdU Imaging Kits, Invitrogen, Waltham, MA, #C10338) was used to assess cell proliferation. HUVEC were incubated with EdU for 2 hours, and stained according to the manufacturer instructions. All fluorescence images were taken using confocal laser scanning microscopy (LSM880, Carl Zeiss).

Migration Assay

For scratch assays, HUVEC were seeded into a six-well plate. A straight line was drawn to create a uniform scratch with a 1-mL pipette tip. After change with fresh media, cells were incubated continuously for 12 hours. Transwell assays were performed as described previously (Corning, Corning, NY, #3464).[29] Three fields of vision were randomly selected using Leica microscopy.

HUVEC Tube Formation Assay

The 96-well plate was precoated with 60 µL of Matrigel (Corning, #354277). When the Matrigel solidified, we added 1×10^4 of a single cell suspension on top of the Matrigel to each well. After 8 hours, three fields of vision were randomly selected using Leica microscopy.

Protein Extraction and Western Blot Analysis

Tissue and cell protein were extracted using a radioimmunoprecipitation assay containing protease inhibitors. After determining protein concentration by the BCA method, Western blot was performed as described elsewhere.[28] Finally, protein bands were visualized by an enhanced chemiluminescence system (Millipore, Burlington, MA). The pools of tissue protein were prepared by mixing six retinas from different mice. All experiments were repeated three times.

Statistical Analysis

All measurements were performed in a blinded manner. All the data were presented as mean ± SEM. The differences between two groups were analyzed by unpaired, two-tailed *t*-test. When there were more than two groups, one-way ANOVA were performed. *P* values of less than 0.05 were considered significant (*$P < 0.05$, **$P < 0.01$, and ***$P < 0.001$). GraphPad prism (Version 7.0; GraphPad Software, San Diego, CA) was used to conduct all statistical analyses.

Results

KC7F2 Attenuated Pathological RNV in OIR Models

To investigate the retinal vessels, whole-mounted retinas were immunofluorescence stained with CD31 (Figs. 1A, 2A, upper image), and higher magnification images were shown (Figs. 1A, 2A, lower image). Unlike the normal retinal vasculature in control group, neovascular (filled with yellow) and avascular areas (outlined with white lines) could be observed in retinas of rodent OIR models. After the KC7F2 intervention, retinal neovascular area was reduced in rat OIR model (Fig. 1B) and mouse OIR model (Fig. 2D), while avascular area did not change in either the rat or mouse OIR models (Figs. 1C, 2E). Similar results were shown in CD31 staining of frozen sections (Figs. 2C, G). To further identify the antiangiogenic effect of KC7F2, HE-stained paraffin sections were performed to count neovascular cell nuclei anterior to the internal limiting membrane (Fig. 2B). Results showed that the number of neovascular cell nuclei anterior to the internal limiting membrane in the OIR + KC7F2 group was less than that in OIR group (Fig. 2F). All these results revealed that KC7F2 attenuated pathological RNV in rodent OIR models, but did not affect physiologic retinal revascularization.

KC7F2 Inhibited Increased Endothelial Cell Proliferation But Did Not Affect Apoptosis

To determine an appropriate concentration of KC7F2 for cell experiment, a CCK8 assay was used for the analysis of cytotoxicity. HUVEC were treated with different concentrations of KC7F2 (0, 0.1, 1, 10, 50, and 100 µM) for 24 hours (Fig. 3A). The results showed that KC7F2 at concentration of 10 µM was not cytotoxic, which was used in all

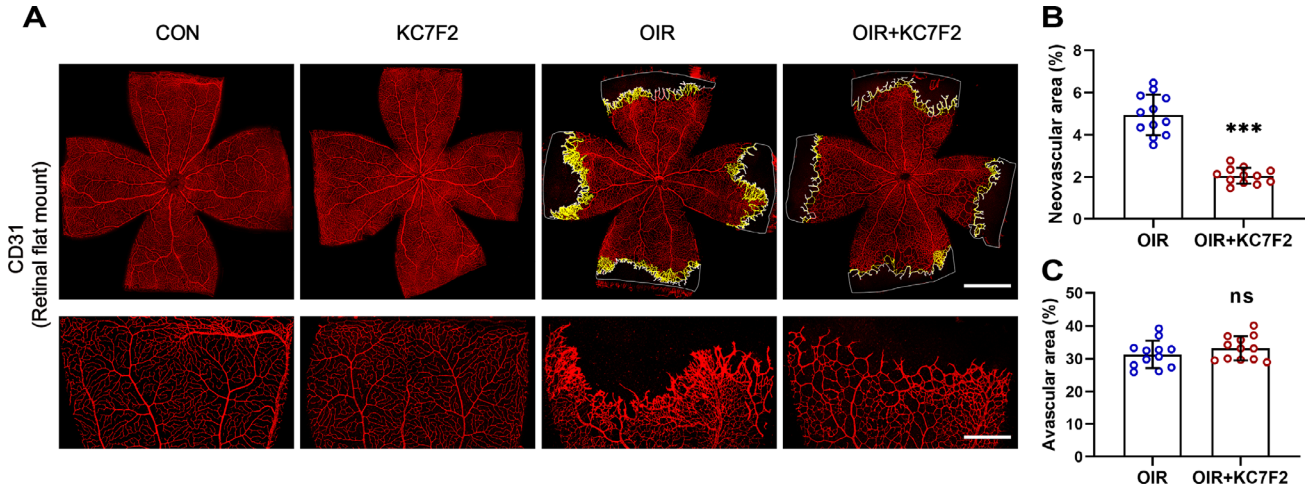

Figure 1. The effect of KC7F2 on pathological RNV in retina of OIR rats. (**A, Upper image**) Retinas of rats from control group, KC7F2 group, OIR group and OIR+KC7F2 group were harvested at P18 and subjected to whole-mount immunostaining with CD31 (red), showing neovascular areas (filled with *yellow*) and avascular areas (outlined with *white lines*). Scale bar, 1 mm. (**A, Lower image**) The high power images from each group were shown. Scale bar, 300 µm. (**B**) Neovascular areas and (**C**) avascular areas were quantified ($n = 12$). The graphs are presented as mean ± SEM. ***$P < 0.001$; ns, no statistical significance. CON, control.

Investigative Ophthalmology & Visual Science

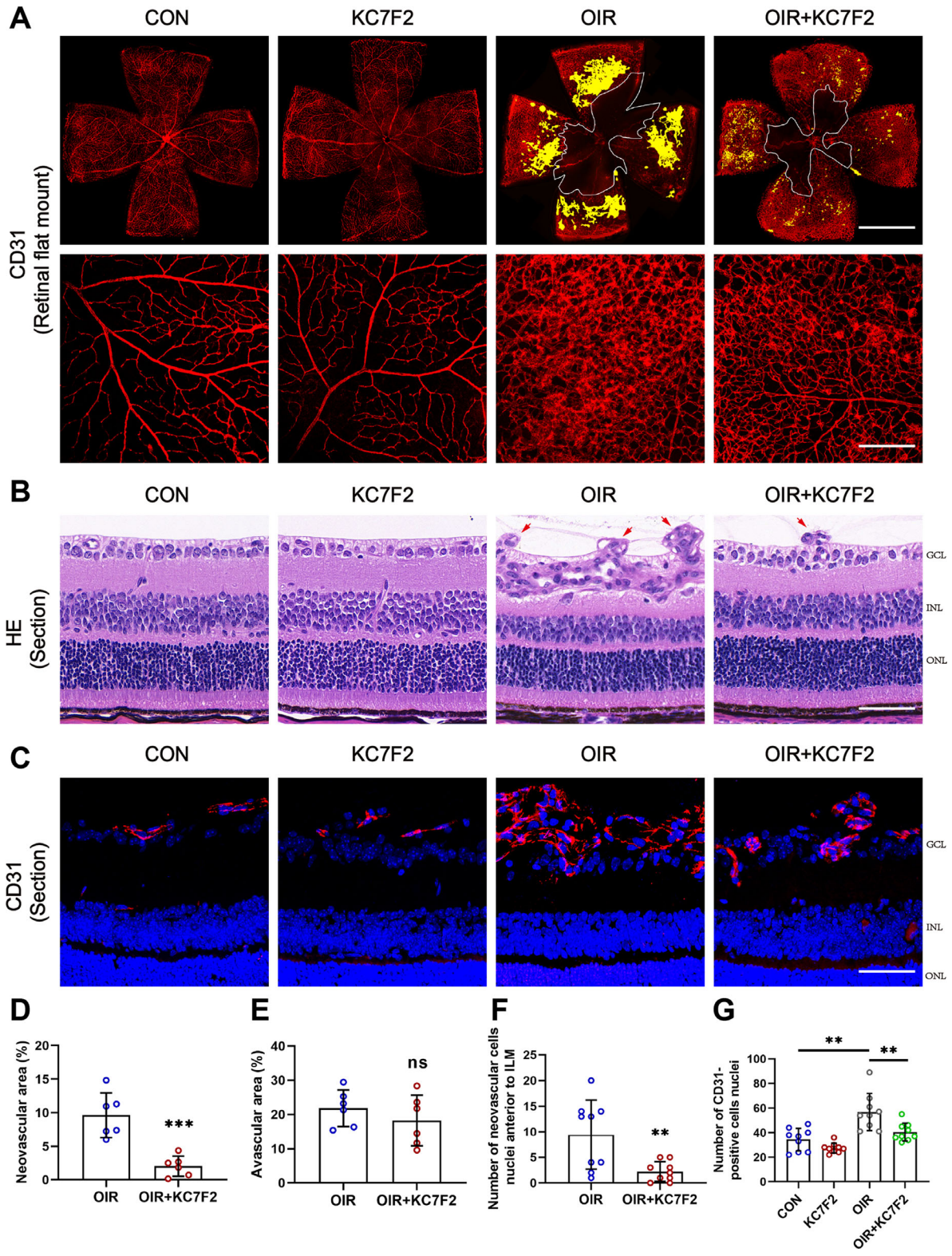

Figure 2. The effect of KC7F2 on pathological RNV in OIR mice retina. (**A, Upper image**) Mice retinas from the control group, KC7F2 group, OIR group, and OIR+KC7F2 group were harvested at P17 and subjected to whole-mount immunostaining with CD31 (*red*), showing neovascular areas (filled with *yellow*) and avascular areas (outlined with *white* lines). Scale bar, 500 µm. (**A, Lower image**) The high power images from each group were shown. Scale bar, 100 µm. (**D**) Neovascular areas and (**E**) avascular areas were quantified ($n = 6$). (**B**) Neovascular cell nuclei anterior to internal limiting membrane (ILM) represented extent of RNV. The *arrows* denote neovascular tufts. Scale bar, 50 µm. (**F**) Quantification of the neovascular cell nuclei anterior to the ILM in OIR group and OIR+KC7F2 group at P17 ($n = 9$). (**C**) Representative image of immunofluorescent staining with CD31 (*red*) in each group. The nuclei were stained with 4′,6-Diamidino-2-phenylindole (DAPI) (*blue*). Scale bar, 50 µm. (**G**) Quantification of CD31-positive cells nuclei in each group at P17 (n = 9). The graphs are presented as mean ± SEM. GCL, ganglion cell layer; INL, inner nuclear layer; ONL, outer nuclear layer. $^{**}P < 0.01$; $^{***}P < 0.001$. CON, control; ns, no statistical significance.

Investigative Ophthalmology & Visual Science

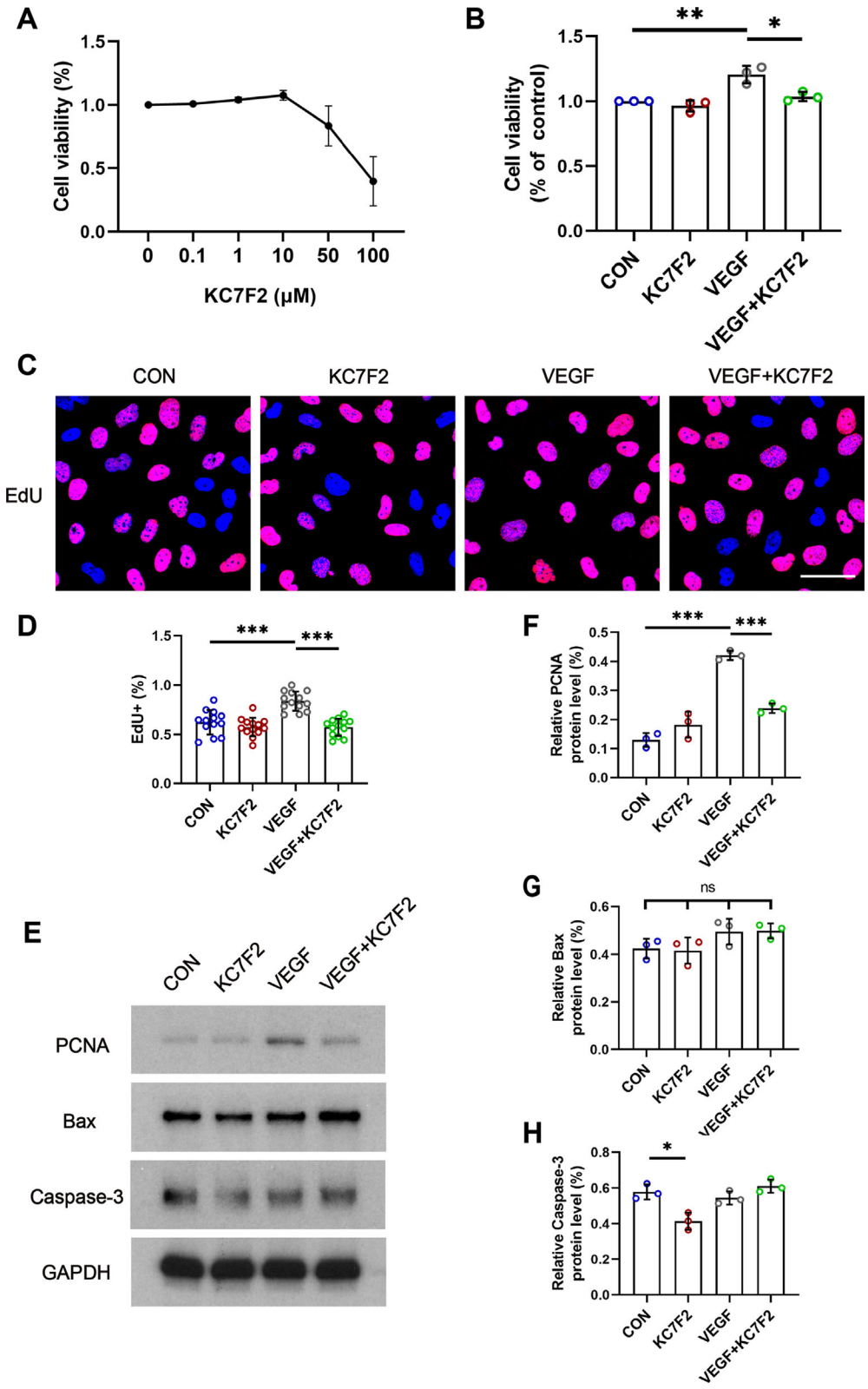

Figure 3. The effect of KC7F2 on cell proliferation in VEGF-induced HUVEC. (**A**) Cytotoxicity analysis via the CCK8 assay. HUVEC were treated with different concentrations of KC7F2 (0, 0.1, 1, 10, 50, and 100 μM) for 24 h. The control group was set at 1.0. (**B**) The effect of KC7F2 on VEGF-induced cytotoxicity of HUVEC was measured by CCK8 assay. The control group was set at 1.0. (**C**) Representative image of EdU incorporation assay in each group. EdU staining (*red*) showed the effects of 10 μM KC7F2 on VEGF-induced proliferation of HUVEC. Scale bar, 50 μm. (**D**) Percentage of EdU-positive cells was quantified. (**E**) Western blot showed the expression of PCNA, Bax and Caspase-3 in each group. GAPDH served as the loading control. (**F–H**) The histogram showed the densitometric analysis of the average levels of PCNA, Bax, and Caspase-3 to GAPDH. The graphs are presented as mean ± SEM of three independent experiments. $^{*}P < 0.05$; $^{**}P < 0.01$; $^{***}P < 0.001$, CON, control; ns, no statistical significance.

Investigative Ophthalmology & Visual Science

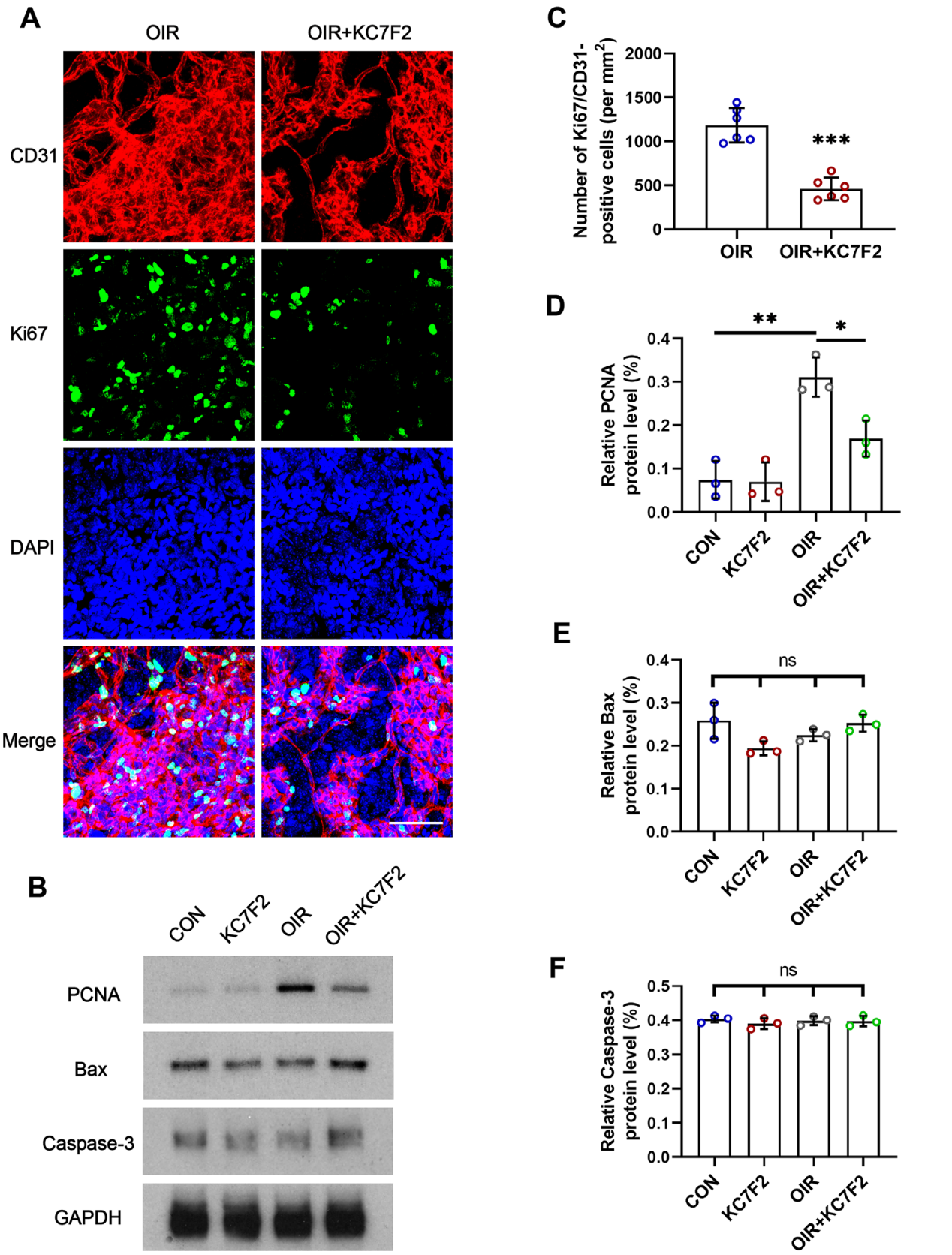

Figure 4. The effect of KC7F2 on endothelial cell proliferation in OIR mice retina. (**A**) Representative images of immunofluorescent staining with CD31 (*red*) and Ki67 (*green*) in each group. The nuclei were stained with 4′,6-Diamidino-2-phenylindole (DAPI) (*blue*). Scale bar, 50 µm. (**C**) Quantification of the Ki67-positive cells in the neovascularized areas ($n = 6$). (**B**) Western blot showed the expression of PCNA, Bax, and Caspase-3 in each group. GAPDH served as the loading control. (**D–F**) The histogram showed the densitometric analysis of the average levels of PCNA, Bax, and Caspase-3 to GAPDH ($n = 3$). The graphs are presented as mean ± SEM. *$P < 0.05$; **$P < 0.01$; ***$P < 0.001$. CON, control; ns, no statistical significance.

Investigative Ophthalmology & Visual Science

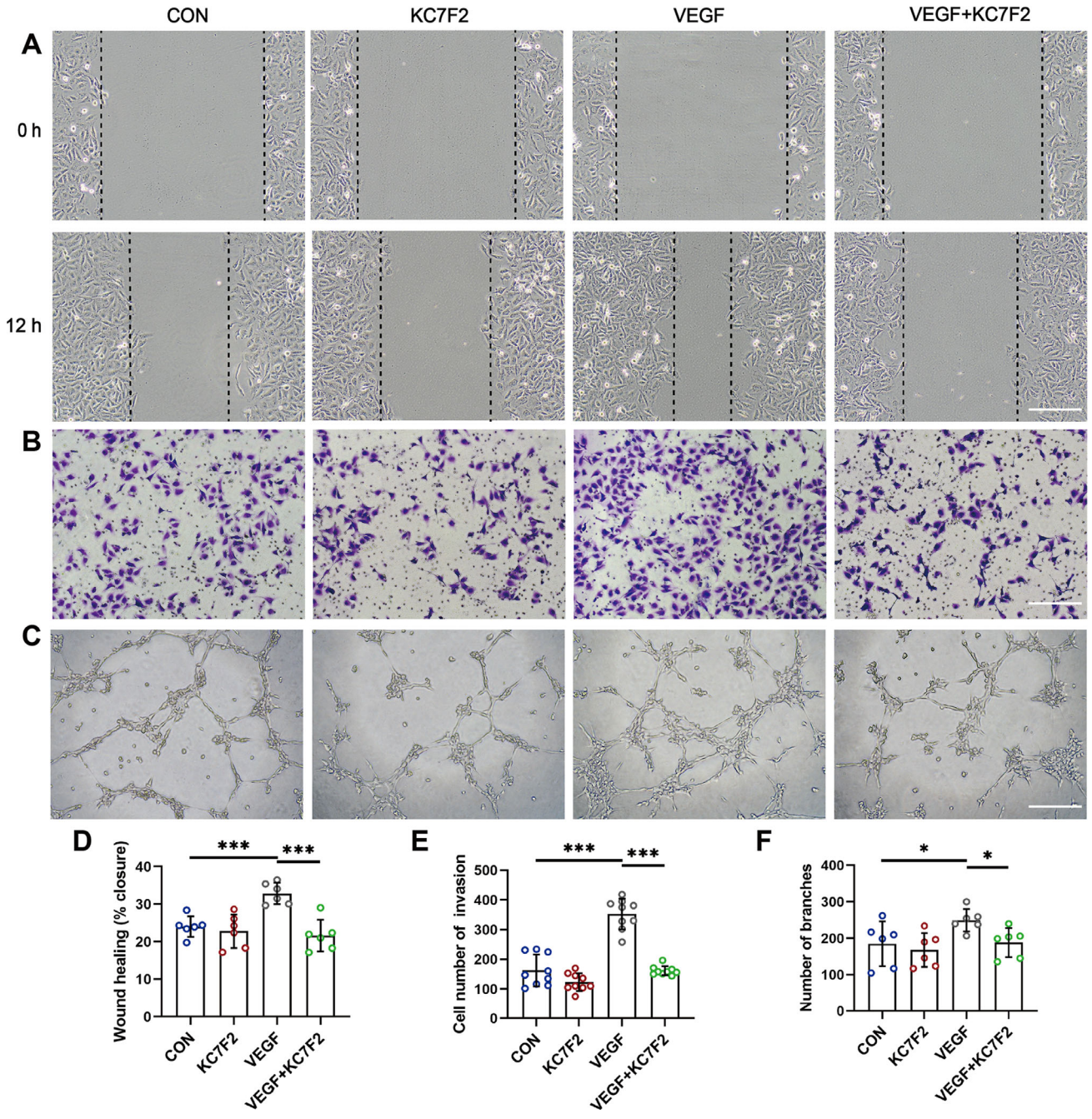

Figure 5. The effect of KC7F2 on migration and tube formation in VEGF-induced HUVEC. (**A**) Representative photomicrographs of scratch assay in each group for 0 and 12 hours. Scale bar, 1 mm. (**D**) Wound healing (percent closure) was quantified. (**B**) Representative photomicrographs of transwell migration assay in each group. Scale bar, 1 mm. (**E**) Number of HUVEC was counted on the lower surface of the transwell membrane in each group. (**C**) Representative photomicrographs of HUVEC tube formation assay in each group. Scale bar, 1 mm. (**F**) Number of branches in each group were quantified. The graphs are presented as mean ± SEM of three independent experiments. $^{*}P < 0.05$; $^{***}P < 0.001$. CON, control.

subsequent in vitro experiments. In a CCK8 cell proliferation assay, KC7F2 treatment inhibited cell proliferation in VEGF-induced HUVEC and did not affect that in the control group (Fig. 3B). Similar results were showed in EdU incorporation assay (Figs. 3C, D). To further confirm this result, a Western blot was conducted to measure the expression of proliferating cell nuclear antigens (PCNAs) (Fig. 3E), a marker of cell proliferation. The results showed that PCNA expression increased in VEGF group, and this trend was suppressed by KC7F2 treatment (Fig. 3F). These results revealed that KC7F2 inhibited VEGF-induced endothelial cell proliferation.

Next, we investigated the effect of KC7F2 on endothelial cell proliferation in OIR mice retina. As shown in Figure 4A, the density of Ki67+/CD31+ cells colocalizing neovascular areas in the retina of OIR group was higher compared with the OIR + KC7F2 group (Fig. 4C). Western blot (Fig. 4B) showed that the level of PCNA expression increased in OIR group, and this trend was suppressed by KC7F2 treatment (Fig. 4D). Meanwhile, KC7F2 treatment did not decrease the level of PCNA protein in normoxia-treated mice, indicating that KC7F2 did not affect physiologic retinal endothelial cell proliferation. These results suggested that KC7F2 especially

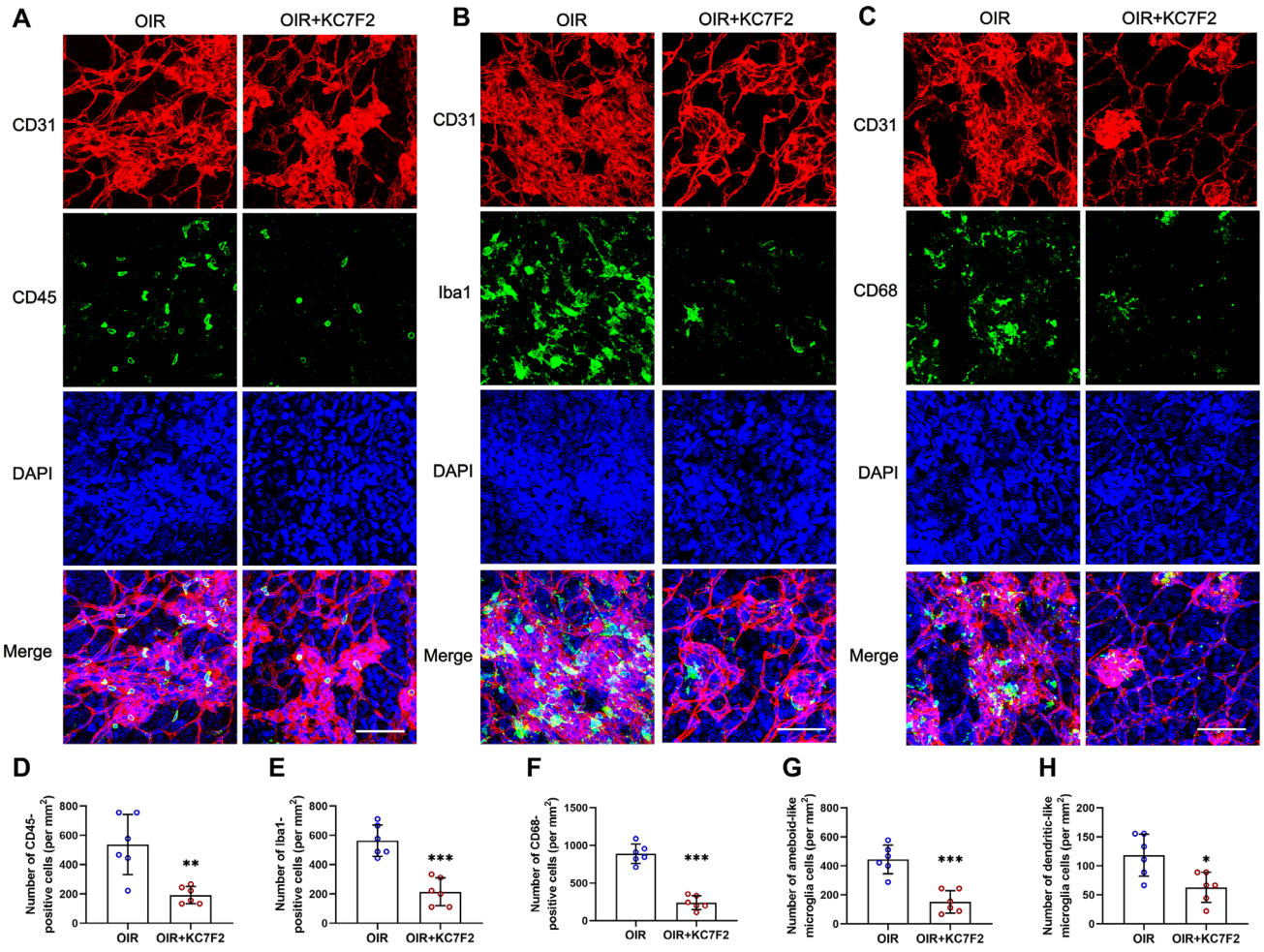

Figure 6. The effect of KC7F2 on inflammatory in OIR mice retina. (**A**) Representative images of immunofluorescent staining with CD31 (*red*) and CD45 (*green*) in each group. The nuclei were stained with 4′,6-Diamidino-2-phenylindole (DAPI) (*blue*). Scale bar, 50 µm. (**D**) Quantification of the CD45-positive cells in the neovascularized areas ($n = 6$). (**B**) Representative images of immunofluorescent staining with CD31 (*red*) and Iba1 (*green*) in each group. The nuclei were stained with DAPI (*blue*). Scale bar, 50 µm. (**E**) Quantification of the Iba1-positive cells in the neovascularized areas ($n = 6$). (**G**) Quantification of ameboid-like microglia cells ($n = 6$). (**H**) Quantification of dendritic-like microglia cells ($n = 6$). (**C**) Representative images of immunofluorescent staining with CD31 (*red*) and CD68 (*green*) in each group. The nuclei were stained with DAPI (*blue*). Scale bar, 50 µm. (**F**) Quantification of the CD68-positive cells in the neovascularized areas ($n = 6$). The graphs are presented as mean ± SEM. *$P < 0.05$; **$P < 0.01$; ***$P < 0.001$.

inhibited increased endothelial cell proliferation in retina of OIR mice.

Notably, endothelial cell apoptosis is associated with RNV.[31] We detected the expression of apoptotic-related proteins, Bax and Caspase-3, in the retinas of mice and HUVEC. Except for the decreased expression of Caspase-3 in normal HUVECs treated with KC7F2, the results showed that KC7F2 did not significantly affect the expression of Bax and Caspase-3 (Figs. 3G–H, 4E–F). Summarizing, KC7F2 inhibited increased endothelial cell proliferation, but did not affect apoptosis.

KC7F2 Inhibited Migration and Tube Formation in VEGF-Induced HUVEC

Scratch and transwell assays were performed to determine whether cell migration was modified by KC7F2. As presented in Fig. 5A, the migratory responses in VEGF-treated HUVEC were markedly increased compared with untreated HUVEC, whereas KC7F2 inhibited this VEGF-induced migratory response (Fig. 5D). Transwell assays showed the same trend as scratch assays (Figs. 5B, E). The effect of KC7F2 on the tube formation ability of HUVEC was determined in a tube formation assay (Fig. 5C). The results revealed that KC7F2 significantly decreased VEGF-induced HUVEC tube formation performed by counting branch points (Fig. 5F). Overall, KC7F2 exerted an inhibitory effect on the migration and tube formation ability of VEGF-induced HUVEC.

KC7F2 Decreased Retinal Inflammation in OIR Mice

It is widely recognized that vascular inflammation is closely linked to neovascularization.[32] Therefore, we investigated inflammatory cells on the neovascular areas in the retinas of the OIR group. Immunofluorescence results showed that CD45-positive leukocytes and Iba1-positive microglia were found to colocalize with CD31+ RNV (Figs. 6A-B). After KC7F2 intervention, the density of leukocytes and

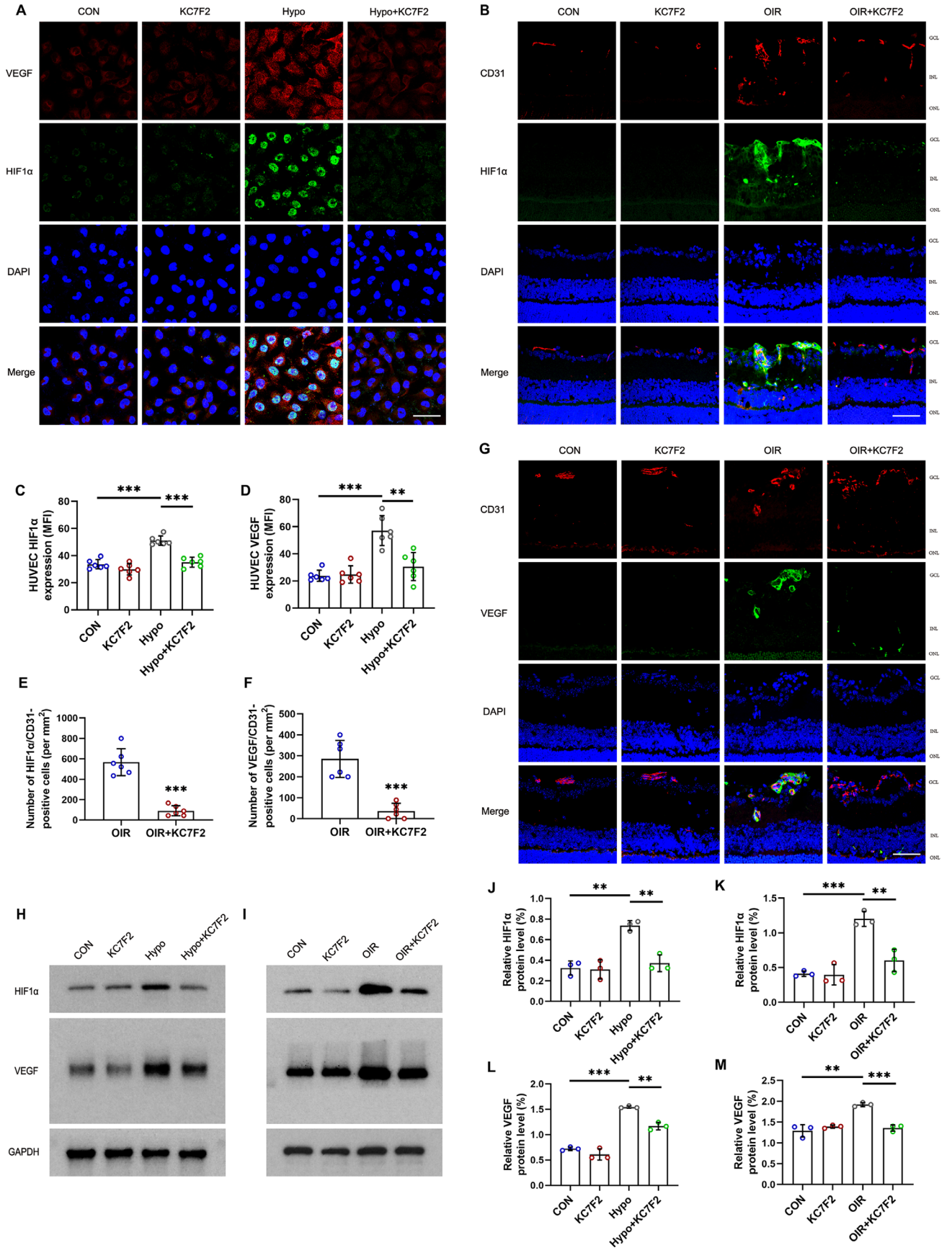

Figure 7. The effect of KC7F2 on HIF1α-VEGF pathway in vivo and in vitro. (**A**) Representative images of immunofluorescent staining with VEGF (*red*) and HIF1α (*green*) in each group. The nuclei were stained with 4′,6-Diamidino-2-phenylindole (DAPI) (*blue*). Scale bar, 50 µm. (**C**, **D**) The histogram showed mean fluorescence intensity (MFI) of HIF1α, VEGF ($n = 6$). (**B**) Representative images of immunofluorescent

staining with CD31 (*red*) and HIF1α (*green*) in each group. The nuclei were stained with DAPI (*blue*). Scale bar, 50 µm. (**E**) Number of HIF1α/CD31-positive cells was quantified ($n = 6$). (**G**) Representative images of immunofluorescent staining with CD31 (*red*) and VEGF (*green*) in each group. The nuclei were stained with DAPI (*blue*). Scale bar, 50 µm. (**F**) Number of VEGF/CD31-positive cells was quantified ($n = 6$). (**H**) Western blot showed the expression of HIF1α, VEGF in each group. (**J**, **K**) The histogram showed the densitometric analysis of the average levels of HIF1α, VEGF to GAPDH. (**I**) Western blot showed the expression of HIF1α, VEGF in each group. (**L**, **M**) The histogram showed the densitometric analysis of the average levels of HIF1α, VEGF to GAPDH. The graphs are presented as mean ± SEM. $^{*}P < 0.05$; $^{**}P < 0.01$; $^{***}P < 0.001$.

microglia colocalizing on the neovascular areas decreased significantly (Figs. 6D, E). The morphology of microglia could change from a dendritic morphology to an amoeboid morphology when activated.[33] The density of dendritic and ameboid microglia in the neovascular area were counted separately based on the same statistical approach in our previous work.[34] We found that the density of dendritic and ameboid microglia in neovascular area both decreased in the OIR + KC7F2 group (Figs. 6G-H). Meanwhile, we added immunofluorescent staining with CD68 (Fig. 6C), a marker for activated microglia and macrophages.[35] Results showed that the density of CD68 colocalizing on the neovascular areas decreased significantly in the OIR + KC7F2 group (Fig. 6F). These results suggested that KC7F2 treatment decreased retinal inflammation in OIR mice.

KC7F2 Inhibited the HIF1α-VEGF Pathway In Vivo and In Vitro

HIF1α–VEGF signaling is a critical regulator of pathologic RNV. To determine the effect of KC7F2 on the expression levels of HIF1α and VEGF in vitro, HUVEC were subjected to hypoxia (1% O_2) for 12 hours. Immunofluorescent staining (Fig. 7A) showed that the fluorescence of HIF1α and VEGF was relatively weak in normoxic HUVEC, regardless of KC7F2 treatment. But it was strongly enhanced under hypoxic conditions, then diminished by KC7F2 intervention (Figs. 7C, D). As shown in Figure 7H, Western blot showed that KC7F2 did not affect physiological HIF1α and VEGF expression in HUVEC in the control group and validated the effect of KC7F2 inhibiting HIF1α-VEGF pathway activation in hypoxia-induced HUVEC (Figs. 7J, L).

Next, we further investigated the impact of KC7F2 on the HIF1α-VEGF signaling pathway in OIR mice. A Western blot analysis (Fig. 7I) and immunofluorescent staining (Figs. 7B, G) were used to detect the expression of HIF1α-VEGF in the retina of different groups. HIF1α and VEGF, colocalizing with CD31+ endothelial cells, were significantly upregulated in the OIR group and downregulated by the KC7F2 intervention compared with OIR group (Figs. 7E, F, K, M). No significant differences in HIF1α and VEGF expression were observed between control group and KC7F2 group (Fig. 7K). Taken together, KC7F2 inhibited the HIF1α-VEGF pathway in vivo and in vitro, and this inhibition effect was absent in normoxic environment.

Discussion

As a neovascular retinal disease, the pathogenesis of ROP has not been elucidated fully.[4] Studies have confirmed that oxygen plays a pivotal role in the formation of RNV in ROP.[5,7] Based on this finding, the mouse OIR model is widely accepted for the study of ROP.[36] However, there are limitations to this model. The mouse OIR model is a vascular wound healing model where the central retinal vessels are obliterated.[36] This model differs from pathological mechanism of ROP, where the peripheral retinal vessels fail to develop.[4] Nonperfused zones were presented in the peripheral retina in the rat ROP model developed by Penn et al.,[27] which is similar to the ROP and selected for additional experimentation. In this study, we injected KC7F2 intraperitoneally in the rodent OIR models, finding that RNV was suppressed significantly. Consistent with our study, previous studies have found that KC7F2 could inhibit angiogenesis in colorectal cancer[37] and attenuate the remodeling of aorta in mice exposed to intermittent hypoxia.[25] Of note, KC7F2 had no significant effect on the size of avascular areas, suggesting that this antiangiogenic effect targeted only abnormal neovascularization, rather than the repair of normal retinal vasculature.

Next, we explored the specific mechanism underlying the antiangiogenic effects of KC7F2. The process of neovascularization depends on the proliferation of vascular endothelial cells.[38] Our findings revealed that KC7F2 inhibited increased cell proliferation in VEGF-induced HUVEC and attenuated pathological RNV in OIR mice by inhibiting the proliferation of endothelial cells in the neovascular areas. Also, preventing endothelial cell from undergoing apoptosis can decrease capillary loss and subsequent neovascularization.[31] However, the results showed that KC7F2 had no effect on the apoptosis of endothelial cells. Biological functions of endothelial cells, such as tube formation and migration, also play an important role in RNV.[5] Our results suggested that KC7F2 suppressed the migration and tube formation of endothelial cells, which could further explain the antiangiogenic effect of KC7F2. However, HUVEC derived from a macrovascular bed are different from microvascular endothelial cells.[39] It should be noted that it must be cautious to extend the conclusion from HUVEC to retinal microvascular endothelial cells.

Inflammation is often accompanied by neovascularization, and they influence and promote each other.[32,40] On the one hand, there are abundant inflammatory cell infiltration in the retina of ROP (e.g., leukocytes[41] and microglia[42]). Inflammatory factors secreted by inflammatory cells can act on vascular endothelium and participate in pathological RNV.[43] On the other hand, pathological RNV lacks an intact blood–retinal barrier, which leads to plasma extravasations and tissue edema, further exacerbating inflammation of the retina.[44] As a component of inflammatory responses, knockout of HIF1α in macrophages and neutrophils inhibited glycolysis, leading to an attenuated inflammatory response.[45] This finding might suggest that HIF1α inhibitors have the ability to inhibit inflammation. Recent studies provided evidence that KC7F2 decreased the inflammatory response in human monocytic cells[46] and microglial cells.[47] In the present study, our results showed that KC7F2 significantly decreased the density of leukocytes and microglia in the neovascular areas of OIR mice retina. These results suggested that KC7F2 had potential anti-inflammatory effect on retinas, which may be a complementary mechanism of inhibiting RNV.

Investigative Ophthalmology & Visual Science

The HIF1α–VEGF pathway is directly related to the pathogenesis of ROP.[8] HIF1α is a major transcriptional factor in adaptive responses to hypoxia, which upregulates several proangiogenic growth factors including VEGF, such as angiopoietin 2, vascular endothelial–protein tyrosine phosphatase, stromal-derived growth factor, placental growth factor.[7] VEGF, in combination with angiopoietin 2 and vascular endothelial–protein tyrosine phosphatase, causes the sprouting of new vessels,[48] acting together with stromal-derived growth factor and placental growth factor to recruit bone marrow–derived cells, which provide paracrine stimulation.[49] A previous study reported that intravitreal injections of adenovirus vector overexpressing HIF1α elicited a strong increase in RNV,[50,51] indicating that HIF1α held a critical position in the formation of RNV. Furthermore, mice with conditional deletion of HIF1α in astrocytes exhibited decreased RNV,[52] and targeting HIF1α decreased hypoxic-induced cone degeneration and prevented subretinal neovascularization.[53] Hence, we speculate that HIF1α is an attractive target for pathological RNV therapy, which has its own features compared with anti-VEGF therapy. This study focused on KC7F2, a small molecule compound that can inhibit the translation of HIF1α. Our research confirmed that KC7F2 significantly decreased expression of HIF1α and VEGF in endothelial cells both in vitro and in vivo. It can be inferred that KC7F2 exerts its antiangiogenic effect mainly via HIF1α-VEGF pathway.

It is worth noting that HIF1α not only affects the development of physiological retinal vessels, but also plays a role in cell metabolism, immune response, and other physiological processes.[16,54] The embryonic lethal phenotype of HIF1α knock-out mice (HIF1$\alpha^{-/-}$)[55] indicated that HIF-target therapy had potential safety issues, which was the focus of our investigation. In this study, the KC7F2 therapeutic control groups were set up to evaluate the safety of KC7F2 treatment. The pups treated with KC7F2 showed no decrease in body weight (Supplementary Fig. S1C, D), with no abnormal findings in retinal morphology. And KC7F2 did not impair the proliferation, migration, or tube formation ability of HUVEC in normoxic environments. No marked toxicities or adverse effects were observed in vitro or in vivo. According to the literature, HIF1α can be inactivated safely in cones, rods,[56,57] and HIF1α knockdown in the peripheral retina,[58] Müller cells,[59] and astrocytes,[52] did not exhibit abnormal retinal architecture. However, Caprara et al.[58] found that HIF1α was required for the formation of the intermediate plexus in retina. Those potential risks of HIF1α-targeted therapies might be derived from downregulated HIF1α expression, which could not meet basic physiological requirements. Notably, our study found that KC7F2 did not decrease physiological HIF1α expression in normal retina, which suggested that KC7F2 might be a safer and milder treatment. However, considering that preterm infants are different from adults, the safety of KC7F2 and the role of HIF1α in retinal development were needed to be explored further.

In conclusion, our current study exhibited that KC7F2 could attenuate RNV and inflammatory responses, possibly via inhibiting HIF1α and VEGF signaling pathway. These results suggested that KC7F2 might be considered as a potent drug for the treatment of ROP.

Acknowledgments

Supported by the National Natural Science Foundation of China (81870668), the Young Scientists Fund of the National Natural Science Foundation of China (81900864), and the Research Grant from Guangzhou Municipal Science and Technology Bureau in China (202102010324).

Disclosure: **X. Tang**, None; **K. Cui**, None; **X. Lu**, None; **P. Wu**, None; **S. Yu**, None; **B. Yang**, None; **Y. Xu**, None; **X. Liang**, None

References

1. Hartnett ME, Penn JS. Mechanisms and management of retinopathy of prematurity. *N Engl J Med*. 2012;367:2515–2526.
2. Hellstrom A, Smith LE, Dammann O. Retinopathy of prematurity. *Lancet*. 2013;382:1445–1457.
3. Holmstrom G, Hellstrom A, Granse L, et al. New modifications of Swedish ROP guidelines based on 10-year data from the SWEDROP register. *Br J Ophthalmol*. 2020;104:943–949.
4. Hartnett ME. Pathophysiology and mechanisms of severe retinopathy of prematurity. *Ophthalmology*. 2015;122:200–210.
5. Chan-Ling T, Gole GA, Quinn GE, et al. Pathophysiology, screening and treatment of ROP: a multi-disciplinary perspective. *Prog Retin Eye Res*. 2018;62:77–119.
6. Grossniklaus HE, Kang SJ, Berglin L. Animal models of choroidal and retinal neovascularization. *Prog Retin Eye Res*. 2010;29:500–519.
7. Campochiaro PA. Molecular pathogenesis of retinal and choroidal vascular diseases. *Prog Retin Eye Res*. 2015;49:67–81.
8. Penn JS, Madan A, Caldwell RB, et al. Vascular endothelial growth factor in eye disease. *Prog Retin Eye Res*. 2008;27:331–371.
9. Paulus YM, Sodhi A. Anti-angiogenic therapy for retinal disease. *Handb Exp Pharmacol*. 2017;242:271–307.
10. Mehta H, Tufail A, Daien V, et al. Real-world outcomes in patients with neovascular age-related macular degeneration treated with intravitreal vascular endothelial growth factor inhibitors. *Prog Retin Eye Res*. 2018;65:127–146.
11. Ferrara N, Adamis AP. Ten years of anti-vascular endothelial growth factor therapy. *Nat Rev Drug Discov*. 2016;15:385–403.
12. Eadie BD, Etminan M, Carleton BC, et al. Association of repeated intravitreous bevacizumab injections with risk for glaucoma surgery. *JAMA Ophthalmol*. 2017;135:363–368.
13. Yonekawa Y, Wu WC, Nitulescu CE, et al. Progressive retinal detachment in infants with retinopathy of prematurity treated with intravitreal bevacizumab or ranibizumab. *Retina*. 2018;38:1079–1083.
14. Morin J, Luu TM, Superstein R, et al. Neurodevelopmental outcomes following bevacizumab injections for retinopathy of prematurity. *Pediatrics*. 2016;137:e20153218.
15. Maguire MG, Martin DF, Ying GS, et al. Five-year outcomes with anti-vascular endothelial growth factor treatment of neovascular age-related macular degeneration: the comparison of age-related macular degeneration treatments trials. *Ophthalmology*. 2016;123:1751–1761.
16. Semenza GL. Targeting HIF-1 for cancer therapy. *Nat Rev Cancer*. 2003;3:721–732.
17. Pugh CW, Ratcliffe PJ. Regulation of angiogenesis by hypoxia: role of the HIF system. *Nat Med*. 2003;9:677–684.
18. Zhang J, Qin Y, Martinez M, et al. HIF-1alpha and HIF-2alpha redundantly promote retinal neovascularization in patients with ischemic retinal disease. *J Clin Invest*. 2021;131(12):e139202.
19. Saito Y, Uppal A, Byfield G, et al. Activated NAD(P)H oxidase from supplemental oxygen induces neovascularization independent of VEGF in retinopathy of prematurity model. *Invest Ophthalmol Vis Sci*. 2008;49:1591–1598.

20. Stahl A, Connor KM, Sapieha P, et al. Computer-aided quantification of retinal neovascularization. *Angiogenesis*. 2009;12:297–301.
21. Narita T, Yin S, Gelin CF, et al. Identification of a novel small molecule HIF-1alpha translation inhibitor. *Clin Cancer Res*. 2009;15:6128–6136.
22. Koh MY, Spivak-Kroizman TR, Powis G. Inhibiting the hypoxia response for cancer therapy: the new kid on the block. *Clin Cancer Res*. 2009;15:5945–5946.
23. Guan G, Zhang Y, Lu Y, et al. The HIF-1alpha/CXCR4 pathway supports hypoxia-induced metastasis of human osteosarcoma cells. *Cancer Lett*. 2015;357:254–264.
24. Cui W, Xiao Y, Zhang R, et al. SOHLH2 suppresses angiogenesis by downregulating HIF1alpha expression in breast cancer. *Mol Cancer Res*. 2021;19:1498–1509.
25. Liu W, Zhang W, Wang T, et al. Obstructive sleep apnea syndrome promotes the progression of aortic dissection via a ROS- HIF-1alpha-MMPs associated pathway. *Int J Biol Sci*. 2019;15:2774–2782.
26. Xu Y, Lu X, Hu Y, et al. Melatonin attenuated retinal neovascularization and neuroglial dysfunction by inhibition of HIF-1alpha-VEGF pathway in oxygen-induced retinopathy mice. *J Pineal Res*. 2018;64:e12473.
27. Penn JS, Henry MM, Tolman BL. Exposure to alternating hypoxia and hyperoxia causes severe proliferative retinopathy in the newborn rat. *Pediatr Res*. 1994;36:724–731.
28. Huang R, Xu Y, Lu X, et al. Melatonin protects inner retinal neurons of newborn mice after hypoxia-ischemia. *J Pineal Res*. 2021;71:e12716.
29. Xu Y, Yang B, Hu Y, et al. Secretion of Down syndrome critical region 1 isoform 4 in ischemic retinal ganglion cells displays anti-angiogenic properties via NFATc1-eependent pathway. *Mol Neurobiol*. 2017;54:6556–6571.
30. Zhou HJ, Xu Z, Wang Z, et al. SUMOylation of VEGFR2 regulates its intracellular trafficking and pathological angiogenesis. *Nat Commun*. 2018;9:3303.
31. Grant ZL, Whitehead L, Wong VH, et al. Blocking endothelial apoptosis revascularizes the retina in a model of ischemic retinopathy. *J Clin Invest*. 2020;130:4235–4251.
32. Tang J, Kern TS. Inflammation in diabetic retinopathy. *Prog Retin Eye Res*. 2011;30:343–358.
33. Schwabenland M, Brück W, Priller J, et al. Analyzing microglial phenotypes across neuropathologies: a practical guide. *Acta Neuropathol*. 2021;142:923–936.
34. Xu Y, Lu X, Hu Y, et al. Melatonin attenuated retinal neovascularization and neuroglial dysfunction by inhibition of HIF-1α-VEGF pathway in oxygen-induced retinopathy mice. *J Pineal Res*. 2018;64:e12473.
35. Zotova E, Bharambe V, Cheaveau M, et al. Inflammatory components in human Alzheimer's disease and after active amyloid-β42 immunization. *Brain*. 2013;136:2677–2696.
36. Stahl A, Connor KM, Sapieha P, et al. The mouse retina as an angiogenesis model. *Invest Ophthalmol Vis Sci*. 2010;51:2813–2826.
37. Cheng CC, Guan SS, Yang HJ, et al. Blocking heme oxygenase-1 by zinc protoporphyrin reduces tumor hypoxia-mediated VEGF release and inhibits tumor angiogenesis as a potential therapeutic agent against colorectal cancer. *J Biomed Sci*. 2016;23:18.
38. Manavski Y, Lucas T, Glaser SF, et al. Clonal expansion of endothelial cells contributes to ischemia-induced neovascularization. *Circ Res*. 2018;122:670–677.
39. Rezzola S, Belleri M, Gariano G, et al. In vitro and ex vivo retina angiogenesis assays. *Angiogenesis*. 2014;17:429–442.
40. Xu Y, Cui K, Li J, et al. Melatonin attenuates choroidal neovascularization by regulating macrophage/microglia polarization via inhibition of RhoA/ROCK signaling pathway. *J Pineal Res*. 2020;69:e12660.
41. Nakao S, Arima M, Ishikawa K, et al. Intravitreal anti-VEGF therapy blocks inflammatory cell infiltration and re-entry into the circulation in retinal angiogenesis. *Invest Ophthalmol Vis Sci*. 2012;53:4323–4328.
42. Li J, Yu S, Lu X, et al. The phase changes of M1/M2 phenotype of microglia/macrophage following oxygen-induced retinopathy in mice. *Inflamm Res*. 2021;70:183–192.
43. Takeda A, Yanai R, Murakami Y, et al. New insights into immunological therapy for retinal disorders. *Front Immunol*. 2020;11:1431.
44. SanGiovanni JP, Chew EY. The role of omega-3 long-chain polyunsaturated fatty acids in health and disease of the retina. *Prog Retin Eye Res*. 2005;24:87–138.
45. Cramer T, Yamanishi Y, Clausen BE, et al. HIF-1alpha is essential for myeloid cell-mediated inflammation. *Cell*. 2003;112:645–657.
46. Huang X, He Z, Jiang X, et al. Folic acid represses hypoxia-induced inflammation in THP-1 cells through inhibition of the PI3K/Akt/HIF-1alpha pathway. *PLoS One*. 2016;11:e0151553.
47. Rathnasamy G, Ling EA, Kaur C. Hypoxia inducible factor-1alpha mediates iron uptake which induces inflammatory response in amoeboid microglial cells in developing periventricular white matter through MAP kinase pathway. *Neuropharmacology*. 2014;77:428–440.
48. Wakui S, Yokoo K, Muto T, et al. Localization of Ang-1, -2, Tie-2, and VEGF expression at endothelial-pericyte interdigitation in rat angiogenesis. *Lab Invest*. 2006;86:1172–1184.
49. Van Bergen T, Etienne I, Cunningham F, et al. The role of placental growth factor (PlGF) and its receptor system in retinal vascular diseases. *Prog Retin Eye Res*. 2019;69:116–136.
50. Kelly BD, Hackett SF, Hirota K, et al. Cell type-specific regulation of angiogenic growth factor gene expression and induction of angiogenesis in nonischemic tissue by a constitutively active form of hypoxia-inducible factor 1. *Circ Res*. 2003;93:1074–1081.
51. Li HY, Yuan Y, Fu YH, et al. Hypoxia-inducible factor-1alpha: a promising therapeutic target for vasculopathy in diabetic retinopathy. *Pharmacol Res*. 2020;159:104924.
52. Weidemann A, Krohne TU, Aguilar E, et al. Astrocyte hypoxic response is essential for pathological but not developmental angiogenesis of the retina. *Glia*. 2010;58:1177–1185.
53. Barben M, Schori C, Samardzija M, et al. Targeting Hif1a rescues cone degeneration and prevents subretinal neovascularization in a model of chronic hypoxia. *Mol Neurodegener*. 2018;13:12.
54. Weidemann A, Johnson RS. Biology of HIF-1alpha. *Cell Death Differ*. 2008;15:621–627.
55. Ryan HE, Lo J, Johnson RS. HIF-1 alpha is required for solid tumor formation and embryonic vascularization. *EMBO J*. 1998;17:3005–3015.
56. Samardzija M, Barben M, Todorova V, et al. Hif1a and Hif2a can be safely inactivated in cone photoreceptors. *Sci Rep*. 2019;9:16121.
57. Thiersch M, Lange C, Joly S, et al. Retinal neuroprotection by hypoxic preconditioning is independent of hypoxia-inducible factor-1 alpha expression in photoreceptors. *Eur J Neurosci*. 2009;29:2291–2302.
58. Caprara C, Thiersch M, Lange C, et al. HIF1A is essential for the development of the intermediate plexus of the retinal vasculature. *Invest Ophthalmol Vis Sci*. 2011;52:2109–2117.
59. Lin M, Chen Y, Jin J, et al. Ischaemia-induced retinal neovascularisation and diabetic retinopathy in mice with conditional knockout of hypoxia-inducible factor-1 in retinal Muller cells. *Diabetologia*. 2011;54:1554–1566.

Investigative Ophthalmology & Visual Science